

Numerical Study on Diffusion Field as Affected by Arrangement of Supply and Exhaust Openings in Conventional Flow Type Clean Room



S. Murakami, D.Eng.

S. Kato, D.Eng.

Y. Suyama

ABSTRACT

Room air distribution is greatly affected by the arrangement of supply outlets and, possibly, exhaust inlets. The influence of those arrangements on the flow fields is studied here by numerical simulation based on the $k - \epsilon$ two-equation turbulence model. Room airflows in several types of conventional-flow-type clean rooms are analyzed from this point of view.

The flow fields in such rooms as analyzed here are well modeled as serial combinations of "flow units," each of which is composed of one supply jet and the rising streams around it. When the number of supply outlets is decreased, the flow units corresponding to the eliminated supply outlets vanish and the remaining flow units expand. A change in arrangement or in the number of exhaust inlets hardly affects the entire flow field; however, such changes often has a large influence on the contaminant diffusion field.

INTRODUCTION

The conventional-flow-type clean room is now indispensable in many fields of industry for use in quality control. In designing effective contamination control for such clean rooms, an understanding of the flow field itself and of the best means by which to control the resulting diffusion field of contaminant is very important. The airflow pattern in a conventional-flow-type clean room is mainly determined by the shape of the room and by the number of supply outlets. That the flow fields of such clean rooms share many common characteristics, especially when the supply outlets are arranged in the ceiling, is well known. The authors earlier analyzed the flow fields and the resulting diffusion fields of contaminant in typical conventional-flow-type clean rooms (Murakami et al. 1987; Murakami et al. 1988).

This study extends the previous study to analyze the influence of the arrangement of the supply and exhaust openings on the flow fields and diffusion fields using the same and modified types of clean room as were studied before.

In the field of ventilation engineering, the following principles are widely accepted:

1. The exhaust system, including the location of the exhaust opening in a room, has rather small influence on its entire flow field.
2. It does, however, have great influence on the contaminant diffusion field.
3. In contrast to the exhaust system, the supply system—especially the arrangement of the supply openings—has a great influence on the flow field.
4. However, it is the exhaust system, not the supply system, that is mainly responsible for exhausting contaminants.

Because of the last principle, the influence of the arrangement of the supply openings in a room on the contaminant diffusion has not yet been clarified. The aim of this paper is to clarify the influence of the location and the number of such openings both on the room airflow distribution and on the contaminant diffusion in a conventional (turbulent) flow-type clean room.

Numerical simulation of turbulent air flow allows us to precisely analyze the flow and diffusion fields in a room (Murakami et al. 1987). In a preceding study (Murakami et al. 1988), with the simulation based on the $k - \epsilon$ two-equation model, the flow fields and their resulting diffusion fields of contaminant in a conventional-flow-type clean room, whose supply outlets were located on the ceiling, were analyzed precisely. It was shown that the flow and diffusion fields are mainly characterized by serial combinations of "flow units," each composed of an inflow jet and the rising streams around it. The detailed description of "flow unit" is shown in Murakami et al. (1988).

In this study, using the same and modified clean room models as studied before, the influence of the arrangement and number of supply and exhaust openings on the flow and diffusion fields in rooms is analyzed from the viewpoint of flow structure and ventilation efficiency (Kato et al. 1988a).

DIMENSIONLESS STUDY OF CONCENTRATION (MODELS 1 AND 2)

In this study, physical quantities are made dimen-

S. Murakami is Professor and S. Kato is Associate Professor, Institute of Industrial Science, University of Tokyo, Japan; Y. Suyama, formerly Joint Researcher, Institute of Industrial Science, University of Tokyo, is now Researcher, Institute of Technology, Hazama-Gumi Co. Ltd., Japan.

sionless by dividing by representative quantities. The quantities selected are the width of the supply outlet, L_o ; its bulk velocity, U_o ; and the mean contaminant concentration, C_o , averaged over all exhaust inlets. The value of C_o is necessarily equal to the ratio of the contaminant generation rate to the supply air volume rate. The value of C_o may be changed according to the room type in which the ratio of the generation rate to the supply air volume rate may be changed. Thus, two kinds (Models 1 and 2) of dimensionless concentration are used. Model 1 is defined as the concentration non-dimensionalized by the individual C_o of the each room type.

Model 1 is not convenient for comparing the different diffusion fields because the representative value is not common. When we want to compare two dimensionless concentration distribution fields, the value of C_o must be held in common. If the representative concentration used for non-dimensionalizing the concentration is identical, the two dimensionless concentration fields can be compared directly. For this purpose, the value of C_o for the basic type (e.g., Type 4) is used as the common representative concentration. This dimensionless concentration is defined as Model 2. In this case, the two different concentration fields can easily be compared, because the contaminant generation rate is held in common despite the different supply air volume rate.

The two normalization methods of Model 1 and Model 2 become identical in the particular case where the value of C_o , the ratio of the contaminant generation rate to the supply air volume rate, is the same within the different concentration fields to be compared. In this case, the comparison of concentration fields may be conducted by means of Model 1. Conversely, the comparison based on Model 1 may be made on the assumption of the same supply air volume rate and the same generation rate.

MODEL CLEAN ROOMS ANALYZED

Thirteen types of clean rooms are used for analysis in this study. Type 5 through Type 13 are modified from the

previously studied basic types of Type 1 through Type 4 (Murakami et al. 1988). In Table 1, the specifications of these rooms are presented. Figure 1 shows the plans and sections of these 13 types.

1. Type 5 and Type 6: Being derived from Type 1, the height of the exhaust openings is raised. 2. Type 7: Being derived from Type 2, the height of the exhaust openings is also raised. 3. Type 8: Being derived from Type 2, the two diagonal exhaust openings are closed. 4. Type 9: Being derived from Type 3, the two center supply openings are closed. 5. Type 10 through 13: Being derived from Type 4, the supply openings are closed progressively.

Generally, the length and width of the supply outlet, L_o , in a conventional-flow-type clean room is about 0.6 m. The height of the ceiling of the clean room models (4.5 in dimensionless value) in full scale thus corresponds to $4.5 \times 0.6 = 2.7$ m. The source points of contaminant are located under the supply outlet, near the wall, and at the center of the room, respectively. Their height from the floor is set equally at 1.25 in dimensionless value. Another source point of contaminant is located in front of the exhaust inlet, where its height from the floor is 0.5. Since the contaminant in this study is assumed to be of passive scalar quantity, and thus of no effect on momentum equations, its transportation or diffusion is fully controlled by the air flow. Flow fields and resulting diffusion fields are assumed to be in steady states. The contaminant generation rate is also assumed to be constant.

NUMERICAL SIMULATION METHOD

Model equations (3-D $k-\epsilon$ two-equation turbulence model) are given in Table 2. The boundary conditions are tabulated in Table 3. Various types of boundary conditions at the solid wall have been devised, and some of them are shown in Table 4. Some boundary conditions were derived using the concept of log-law (Launder et al. 1974; Chieng et al. 1980; Rodi 1984; cf. Table 4). The solid wall boundary condition derived from the power law of velocity profile is also used (authors cf. Table 4). The latter is very

TABLE 1
Specifications of model clean rooms used

Types of Model Clean Room	Dimension of Plan (#1)	Height of Ceiling (#1)	Number of Supply Outlets	Number of Exhaust Inlets	Supply Air Velocity (#2)	Remarks
TYPE 1	5 X 5	4.5	1	4	1.0	basic type: the smallest room
TYPE 2	8 X 8	4.5	4	4	1.0	basic type
TYPE 3	11 X 8	4.5	6	4	1.0	basic type
TYPE 4	11 X 11	4.5	9	4	1.0	basic type: the largest room
TYPE 5	5 X 5	4.5	1	4	1.0	changing the height of exhaust inlets
TYPE 6	5 X 5	4.5	1	4	1.0	changing the height of exhaust inlets
TYPE 7	8 X 8	4.5	4	2	1.0	2 exhaust inlets are closed
TYPE 8	8 X 8	4.5	4	4	1.0	changing the height of exhaust inlets
TYPE 9	11 X 8	4.5	4	4	1.0	2 supply outlets are closed
TYPE 10	11 X 11	4.5	6	4	1.0	3 supply outlets are closed
TYPE 11	11 X 11	4.5	5	4	1.0	4 supply outlets are closed
TYPE 12	11 X 11	4.5	4	4	1.0	5 supply outlets are closed
TYPE 13	11 X 11	4.5	1	4	1.0	8 supply outlets are closed

*1: dimensionless value (divided by the width of supply outlet L_o (0.6m))
*2: dimensionless value (divided by the supply air velocity V_o (1.0m/s))

simple and has given successful results (Murakami et al. 1987; Murakami et al. 1988). The difference in the simulation results between these log-law types and the power law type is negligible (Kato et al. 1988b; Nagano et al. 1988). In this context, the solid wall boundary condition derived

from the power law of velocity profile is used.

The flow fields in rooms divided into the mesh systems shown in Figure 2 are solved by the finite difference method. The numerical simulation method follows that given in Murakami et al. (1987). After the room flow fields

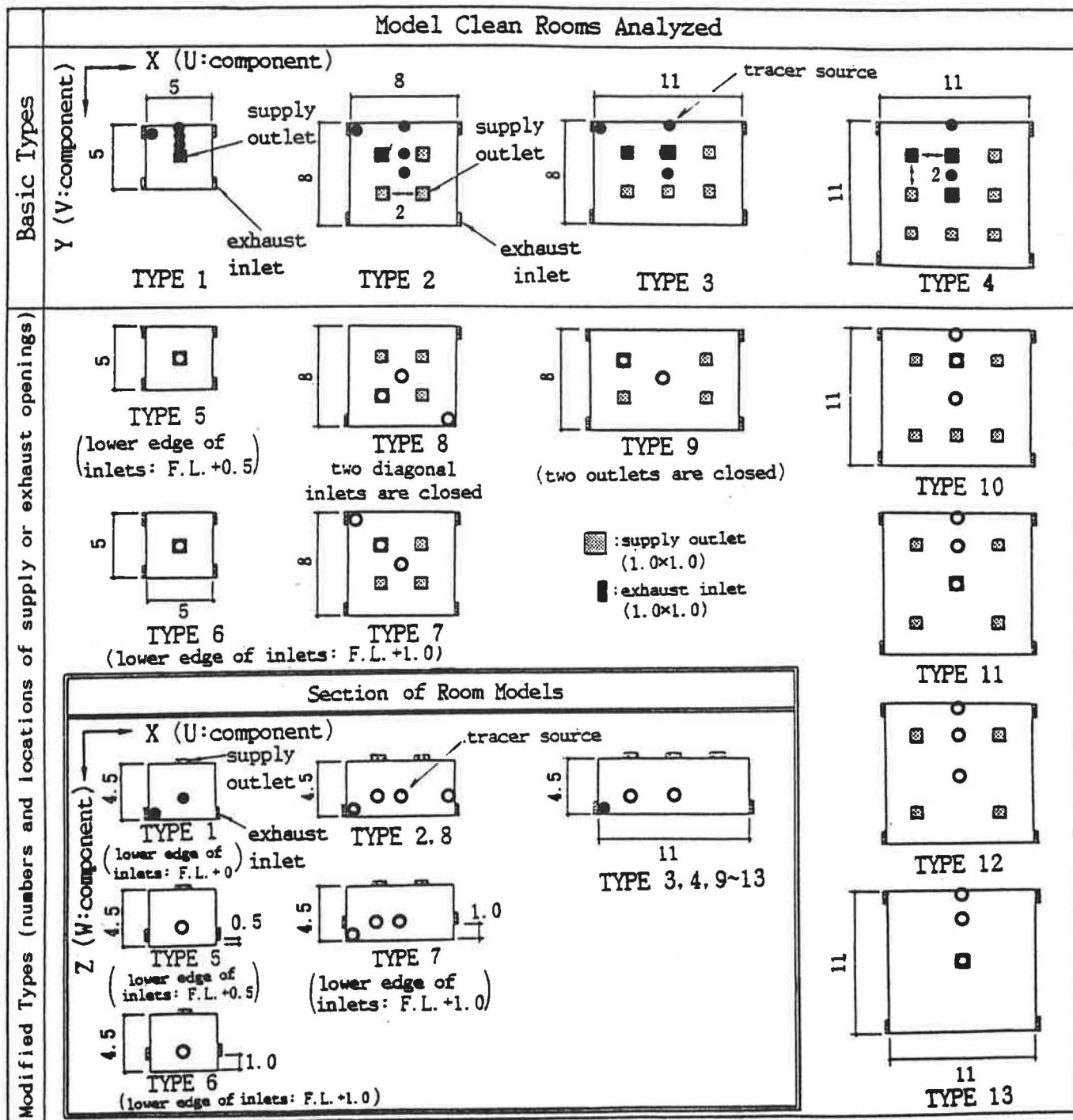


Figure 1 Plans and sections of model clean rooms (Length scale in this figure is nondimensionalized by the width of supply outlet L_0)

are obtained, the contaminant diffusion fields are calculated using such flow field properties as the distribution of velocity vectors and eddy viscosity. The simulated flow fields are not entirely steady and symmetrical due to numerical instability. However, asymmetry of flow fields is very slight and can be disregarded. The calculated contaminant diffusion fields are thus also slightly asymmetric in accord with the flow fields.

ANALYSIS BY MEANS OF NUMERICAL SIMULATION

The correspondence between experiment and numerical simulation is fairly good for both velocity vectors and contaminant concentration in the typical room configurations (Murakami et al. 1987; Murakami et al. 1988). Flow fields and contaminant diffusion fields are therefore analyzed only by numerical simulation in this study. Analysis by simulation is superior to experiment when the purpose is to analyze the resultant influence on the flow and diffusion fields by parametric changes in the flow con-

ditions. In experiments, it is rather difficult to control the flow conditions precisely. For example, one cannot exactly control the uniform distribution of the air supply as well as the exhaust air volume distribution on each exhaust inlet. However, in simulation one can impose any condition with strict exactness. Thus, in this paper, flow fields and contaminant diffusion fields in all the room models are examined only by means of numerical simulation.

EXPRESSION METHODS OF CONTAMINANT DIFFUSION FIELD AND DEFINITION OF SVE1, 2, 3

In this study, contaminant diffusion fields are expressed by four methods:

1. Distribution of contaminant concentration in case of point source: this distribution allows intuitive comprehension of the contaminant diffusion field in a clean room.

2. Spatial average concentration: the first Scale of Ventilation Efficiency (SVE1). This value is proportional to the average time the contaminant is present in the room and indicates how quickly the contaminant generated in the

TABLE 2
Two-Equation Model (Three-Dimensional)

$\frac{\partial U_i}{\partial X_i} = 0$	(1) Continuity equation
$\frac{\partial U_i}{\partial t} + \frac{\partial U_i U_j}{\partial X_j} = - \frac{\partial}{\partial X_i} \left(\frac{P}{\rho} + \frac{2}{3} k \right) + \frac{\partial}{\partial X_j} \left\{ \nu_t \left(\frac{\partial U_i}{\partial X_j} + \frac{\partial U_j}{\partial X_i} \right) \right\}$	(2) Momentum equation
$\frac{\partial k}{\partial t} + \frac{\partial k U_j}{\partial X_j} = \frac{\partial}{\partial X_j} \left(\frac{\nu_t}{\sigma_1} \frac{\partial k}{\partial X_j} \right) + \nu_t S - \varepsilon$	(3) Transport equation for k
$\frac{\partial \varepsilon}{\partial t} + \frac{\partial \varepsilon U_j}{\partial X_j} = \frac{\partial}{\partial X_j} \left(\frac{\nu_t}{\sigma_2} \frac{\partial \varepsilon}{\partial X_j} \right) + C_1 \frac{\varepsilon}{k} \nu_t S - C_2 \frac{\varepsilon^2}{k}$	(4) Transport equation for ε
$\nu_t = k^{1/2} l = \left(C_\mu \frac{k}{\varepsilon} \right)$	(5) Equation for deciding ν_t
$\frac{\partial C}{\partial t} + \frac{\partial C U_j}{\partial X_j} = \frac{\partial}{\partial X_j} \left(\frac{\nu_t}{\sigma_3} \frac{\partial C}{\partial X_j} \right)$	(6) Concentration equation
here $S = \left(\frac{\partial U_i}{\partial X_j} + \frac{\partial U_j}{\partial X_i} \right) \frac{\partial U_i}{\partial X_j}$, $\sigma_1 = 1.0$, $\sigma_2 = 1.3$, $\sigma_3 = 1.0$ $C_\mu = 0.09$, $C_1 = 1.44$, $C_2 = 1.92$	

TABLE 3
Boundary Conditions for Numerical Simulation

(1) Supply Outlet : $U_t = 0.0$, $U_n = U_{out}$, $k = 0.005$, $l = 0.33$, $C = 0.0$ boundary suffix t: tangential component, n: normal component U_{out} : Supply outlet velocity, $U_{out} = 1.0$
(2) Exhaust Inlet : $U_t = 0.0$, $U_n = U_{in}$, $\partial k / \partial Z = 0.0$, $\partial \varepsilon / \partial Z = 0.0$, $\partial C / \partial Z = 0.0$ boundary U_{in} : Exhaust inlet velocity, total exhaust air volume is the same with the total supply air volume, for example in case of TYPE2, 7, 9, 12: $U_{in} = 1.0$
(3) Wall boundary : $\partial U / \partial Z_{z=0} = m U_t z=h / h$, $U_n = 0.0$, $\partial k / \partial Z = 0.0$, $\partial C / \partial Z = 0.0$ $\varepsilon_{z=h} = [C_\mu k_{z=h}^{3/2}] / [C_\mu^{1/4} \kappa h]$ h: Length from the wall surface to the center of the adjacent cell m: 1/7, Power law of profile $U_t \propto Z^m$ is assumed here. κ : 0.4, von Karman constant

TABLE 4
Various solid wall boundary conditions

<p>Log Law Type I (Launder, Spalding)</p>	<p>① $U : \frac{U_1}{\frac{\tau_w}{\rho}} (C_{\mu}^{1/2} \cdot k_1)^{1/2} = \frac{1}{x} \ln \left[\frac{E \cdot h_1 (C_{\mu}^{1/2} \cdot k_1)^{1/2}}{2\nu} \right]$</p> <p style="text-align: right; margin-right: 20px;">$E=9.0$</p> <p>$\left\{ (\nu + \nu_1) \frac{\partial U}{\partial y} \right\}_{y=0} = \frac{\tau_w}{\rho}$</p> <p style="text-align: right; margin-right: 20px;">ν = Molecular kinematic viscosity</p> <p>② $k : \left(\frac{\nu_1}{\sigma_1} \frac{\partial k}{\partial y} \right)_{y=0} = 0$</p> <p style="text-align: right; margin-right: 20px;">suffix 1: value at the center of first fluid cell adjacent to the solid wall</p> <p>$\bar{e}_1 = \frac{C_{\mu}^{1/2} \cdot k_1^{1/2}}{x (h_1/2)} \ln \left[\frac{E \cdot (h_1/2) (C_{\mu}^{1/2} \cdot k_1)^{1/2}}{\nu} \right]$</p> <p>③ $\epsilon : \epsilon_1 = \frac{C_{\mu}^{3/4} \cdot k_1^{3/2}}{x (h_1/2)}$</p>
<p>Log Law Type II (Chieng, Launder)</p>	<p>① $U : \frac{U_1}{\frac{\tau_w}{\rho}} (C_{\mu}^{1/2} \cdot k_v)^{1/2} = \frac{1}{x} \ln \left[\frac{E \cdot h_1 (C_{\mu}^{1/2} \cdot k_v)^{1/2}}{2\nu} \right]$</p> <p>$\left\{ (\nu + \nu_1) \frac{\partial U_1}{\partial y} \right\}_{y=0} = u_*^2 = \frac{\tau_w}{\rho}$</p> <p>$k_v = k_1 + \frac{(k_2 - k_1)}{(h_2 - (h_1/2))} (y_v - (h_1/2))$</p> <p>② $k : \left(\frac{\nu_1}{\sigma_1} \frac{\partial k}{\partial y} \right)_{y=0} = 0$</p> <p>$P_{h_1} = \overline{uv} \frac{\partial U}{\partial y} = \frac{1}{h_1} \int_{y_v}^{h_1} \left[\tau_w + (\tau_e - \tau_w) \frac{y}{h_1} \right] \frac{\partial U}{\partial y} dy$</p> <p>$= \left(\frac{\tau_w}{\rho} \right)^2 \frac{1}{h_1 x \cdot k_1^{1/2}} \ln \left(\frac{h_1}{y_v} \right) + \frac{\tau_w (\tau_e - \tau_w)}{\rho^2 h_1 x \cdot k_1^{1/2}} \left(1 - \frac{y_v}{h_1} \right)$</p> <p>$\bar{e}_1 = \frac{1}{h_1} \cdot 2 \cdot \frac{k_2^{3/2}}{y_v^2} + \frac{1}{h_1 C_L} \left[\frac{2}{3} (k_2^{3/2} - k_1^{3/2}) + 2a (k_2^{1/2} - k_1^{1/2}) + \lambda \right]$</p> <p>$\lambda = a^{3/2} \ln \left[\frac{(k_2^{1/2} - a^{1/2}) / (k_1^{1/2} + a^{1/2})}{(k_1^{1/2} - a^{1/2}) / (k_2^{1/2} + a^{1/2})} \right] \quad (a \geq 0)$</p> <p>$= 2 (-a)^{3/2} \left[\text{TAN}^{-1} \frac{k_2^{1/2}}{(-a)^{1/2}} - \text{TAN}^{-1} \frac{k_1^{1/2}}{(-a)^{1/2}} \right] \quad (a < 0)$</p> <p>here $a = k_1 - \frac{(k_2 - k_1) \cdot h_1}{((h_1/2) - h_2) \cdot 2}$</p> <p>③ $\epsilon : \epsilon_1 = \frac{C_{\mu}^{3/4} \cdot k_1^{3/2}}{x (h_1/2)}$</p>
<p>Log Law Type III (Rodi etc.)</p>	<p>① $U : \frac{U_1}{\frac{\tau_w}{\rho}} (C_{\mu}^{1/2} \cdot k_1)^{1/2} = \frac{1}{x} \ln \left[\frac{E \cdot h_1 (C_{\mu}^{1/2} \cdot k_1)^{1/2}}{2\nu} \right]$</p> <p>$\left\{ (\nu + \nu_1) \frac{\partial U}{\partial y} \right\}_{y=0} = \frac{\tau_w}{\rho}$</p> <p>② $k : k_1 = C_{\mu}^{-1/2} \cdot u_*^2$</p> <p>③ $\epsilon : \epsilon_1 = \frac{u_*^3}{x (h_1/2)}$</p>
<p>Power Law Type (Authors)</p>	<p>① $U : \left(\nu_1 \frac{\partial U}{\partial y} \right)_{y=0} = \nu_1 \cdot \frac{U_1}{(h_1/2)}, n=1/7$</p> <p>② $k : \left(\frac{\nu_1}{\sigma_1} \frac{\partial k}{\partial y} \right)_{y=0} = 0$</p> <p>③ $\epsilon : \epsilon_1 = \frac{C_{\mu}^{3/4} \cdot k_1^{3/2}}{x (h_1/2)}$</p>

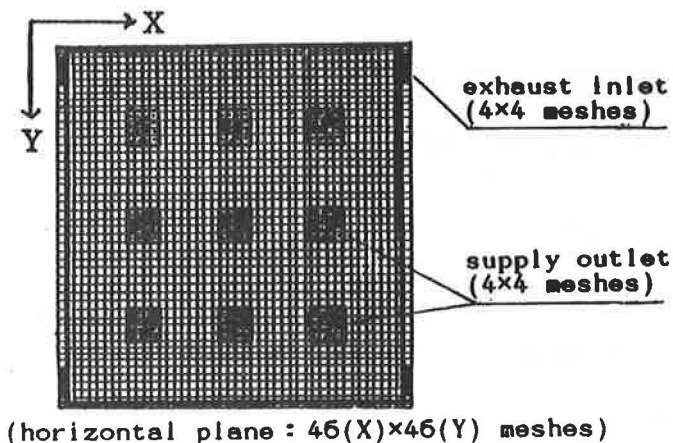


Figure 2 Mesh system (type 4 room model)

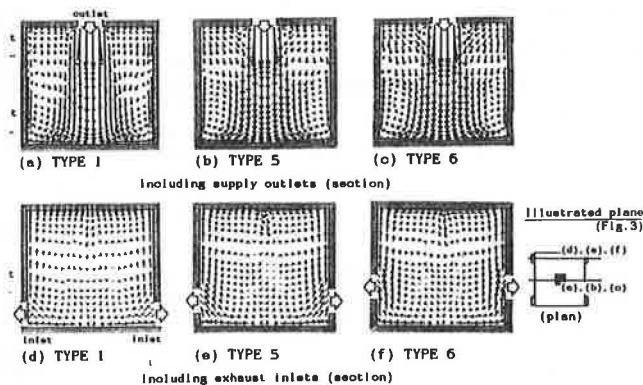


Figure 3 Comparison of velocity vectors in TYPE 1, 5, and 6 (1 outlet & 4 inlets, heights of exhaust inlets are changed)

room is exhausted by the flow field.

3. Mean radius of diffusion: the second Scale of Ventilation Efficiency (SVE2). This value represents the average spatial diffusion.

4. Concentration in case of uniform contaminant generation throughout the room: the third Scale of Ventilation Efficiency (SVE 3). At a given point this value is proportional to the mean traveling time of the supply air to that point. High value for this concentration indicates a high possibility of air contamination, because the air mass must have traveled a long way from the supply outlet.

The details of these scales are described by Kato et al. (1988a).

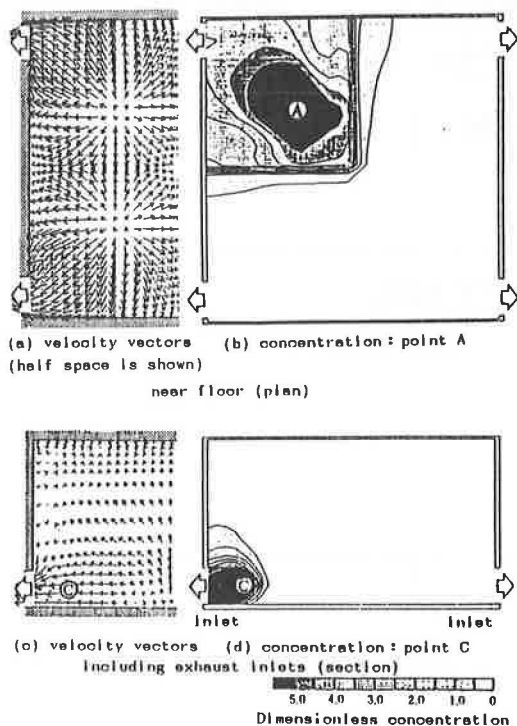


Figure 4 Velocity vectors and contaminant distribution (model 1) in TYPE 2 (4 outlets & 4 inlets)

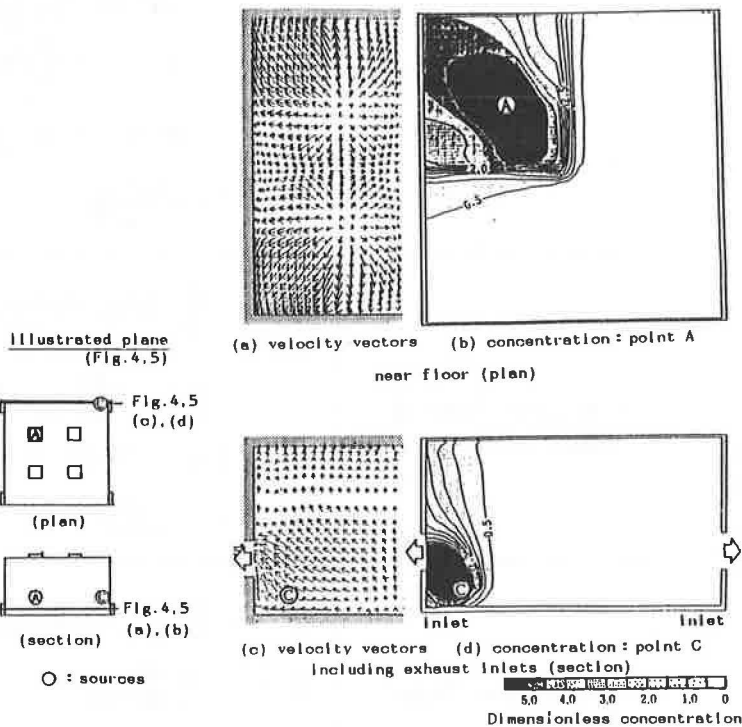


Figure 5 Velocity vectors and contaminant distribution (model 1) in TYPE 7 (4 outlets & 4 inlets, heights of exhaust inlets are changed)

**INFLUENCE OF
ARRANGEMENT OF EXHAUST INLETS**
**Change in the Height of Exhaust Inlets
(Type 1, 5, 6 and Type 2, 7)**

Type 5 and Type 6 are room models derived from Type 1 and are regarded as a sequence in which the height of the floor exhaust inlets in Type 1 are raised. In Type 5 and 6, the exhaust inlets are located 0.5 and 1.0 from the floor, respectively. Type 7 is a room model derived from Type 2, and it, too, is regarded as part of the series in which the height of exhaust inlets in Type 2 is changed. In Type 7, the exhaust inlets are located 1.0 above the floor.

As is shown in Figure 3, the three flow fields of Types 1, 5, and 6 are almost identical. The flow patterns of the jets from the supply outlets, the rising streams beside the walls, and the large recirculating flows around the jets are all very similar.

Figure 4 shows the result of Type 2, which was studied in a previous paper (Murakami et al. 1988). As shown in Figure 5, the characteristics of the flow structure of the four flow units are very similar between Type 2 and Type 7 (Figures 4a and 5a), although there are slight changes, such as rising streams toward the exhaust inlet from the floor and some weak rising streams at the upper position of the exhaust inlet in Type 7 (Figures 4c and 5c). When the contaminant is generated at point C near the exhaust inlet in Type 7 (cf. Figures 4d and 5d), the rising streams near the exhaust inlets transport and diffuse some contaminant. In these figures, dimensionless concentration Model 1 is used. In this case, the contaminant spreads toward the upper area of the exhaust inlet in contrast to Type 2. So in the case of contaminant diffusion with source point C, the values of the spatial average concentration (0.16) and mean radius of diffusion (2.5) in Type 7 are greater than the values in Type 2 (0.06 and 1.7, respectively) for the same generation condition as shown in Table 5. However, this case is the only exception. For the cases of all other contaminant sources, not only the pattern of concentration

distribution but also the values of ventilation efficiency scales (SVE1 and SVE2) are quite similar between Type 2 and Type 7.

Decrease of Exhaust Inlets (Type 2, 8)

Type 8, in which two exhaust inlets are located diagonally, is a room model derived from Type 2 and is regarded as a case of decreasing exhaust inlets. In this room model, only two exhaust inlets are located at diagonal corners (the other two exhaust inlets are eliminated). As shown in Figure 6a, there are four "flow units" in this type as well as in Type 2 (Figure 4a). Since the exhaust air flow rate at each exhaust inlet is greater than for Type 2, the velocity vectors in front of the exhaust inlets become greater than those in Type 2. In the case of contaminant generation at A, which is in the "flow unit" adjacent to the exhaust inlet and is under the supply outlet, although the contaminated space is nearly the same as with Type 2 (cf. Figures 4b and 6b) and the value of the mean radius of diffusion is the same, the value of the spatial average concentration is smaller than that for Type 2, which means that the contaminant is exhausted effectively by the stronger flow toward the exhaust inlet. A comparison of two scales of ventilation efficiency is shown in Table 5.

At the corner of the eliminated exhaust inlets, strong rising streams along the wall appear. When the contaminant is generated in this position (point C), the contaminant spreads upward along the wall and the large area along the ceiling becomes highly contaminated (cf. Figures 6c and 6d). In this case, the values of the average spatial concentration and the mean radius of diffusion are higher than for all other cases in this room model (1.58 and 3.38, respectively). The distribution of the concentration in the case of uniform contaminant generation throughout the room is shown in Figure 7. At the corner near the ceiling of the upper position of the closed exhaust inlets, the concentration becomes very high; the possibility that the air mass in this area will be contaminated should be very high,

TABLE 5
*Values of Spatial Averaged Concentration (SVE1)
and Mean Radius of Diffusion (SVE2) for TYPE 2 ~ TYPE 9*

Scales of Ventilation Efficiency	point A (under supply outlet)		point B (center of room)		point C (at corner of room)	
	Spatial Averaged Concentration	Mean Radius of Diffusion	Spatial Averaged Concentration	Mean Radius of Diffusion	Spatial Averaged Concentration	Mean Radius of Diffusion
	SVE1*1 (Model 1)	SVE2**	SVE1 (Model 1)	SVE2	SVE1 (Model 1)	SVE2
TYPE 2	0.76	3.0	1.50	3.2	0.06	1.7
TYPE 7	0.72	3.0	1.41	3.1	0.16	2.5
TYPE 8	0.60	3.1	1.38	3.2	1.58	3.3
TYPE 3	0.53	2.7	1.72	3.6	0.03	0.13
TYPE 9	1.03	3.5	1.64	3.6	—	—

*1 : These values are made dimensionless by the mean concentration C_0 at all exhaust inlets of each room model respectively. This type of nondimensionalization is defined as Model 1.
*2 : Dimensionless length : these values are made dimensionless by the dividing by the width of the supply outlet (0.6m).

because the high value of this concentration reflects the long traveling time required by an air mass to reach this point from the supply outlets (cf. Kato et al. 1988a).

INFLUENCE OF ARRANGEMENT OF SUPPLY OUTLETS

Decrease of the Number of Supply Outlets (Type 3, 9)

Type 9, in which four supply outlets are located at the ceiling, is a room model derived from Type 3 and is regarded as a case of decreasing supply outlets. In this case, two supply outlets at the center of the room are eliminated. A comparison of Figure 8 with Figure 9 shows that the two flow units corresponding to the eliminated supply outlets vanish, and four flow units corresponding to the supply outlets in the room model appear. Each flow unit occupies a quarter of the room and becomes larger than those of Type 3, where six flow units occupy the same space.

When the contaminant is generated under the supply outlet at point A, the contaminant spreads in the quarter of the room corresponding to that flow unit. In this case, the mean radius of diffusion is 3.5, which is much greater than that in the case of the same contaminant source position in Type 3 (2.7). A comparison between Type 3 and Type 9 is also tabulated in Table 5.

In this study, non-dimensionalized contaminant concentration Model 1 is defined by dividing by the representative contaminant concentration, C_o , which is the mean value of all exhaust inlets. Therefore, actual concentration

is the product of this dimensionless value (Model 1) and the representative concentration, C_o , which is the ratio of the contaminant generation rate to the supply air volume rate. However, to compare the two dimensionless concentration distributions in an equal condition, the representative concentration, C_o , must be held in common between the two. This condition requires that the contaminant generation rate in Type 9 be two-thirds that in Type 3, for the air exchange rate is two-thirds that in Type 3. If a comparison with Type 3 under the same contaminant generation condition is required, both must be normalized by the same representative concentration, C_o , and the value of dimensionless concentration in Type 9 must be multiplied by 1.5. This type of non-dimensional value is defined as Model 2, as mentioned above. Using this procedure, the value of the spatial averaged concentration of Type 9 in the case of source point A (cf. Figures 9b and d) is 1.55(1.03 \times 3/2), which is much greater than the value of Type 3 in the case of the same source point (0.53); this means that Type 9 is inferior to Type 3 in its ability to exhaust contaminant.

At the center of the room, the rising stream appears at the boundary of the flow units. The contaminant generated at source point B (cf. Figure 9f) is transported toward the upper portion of the room and a heavily contaminated region appears near the ceiling. Furthermore, in this case the contaminant spreads throughout the room, and the value of the mean radius of diffusion becomes greater (3.6). The values of the ventilation efficiency (SVE1 and SVE2) are tabulated in Table 5.

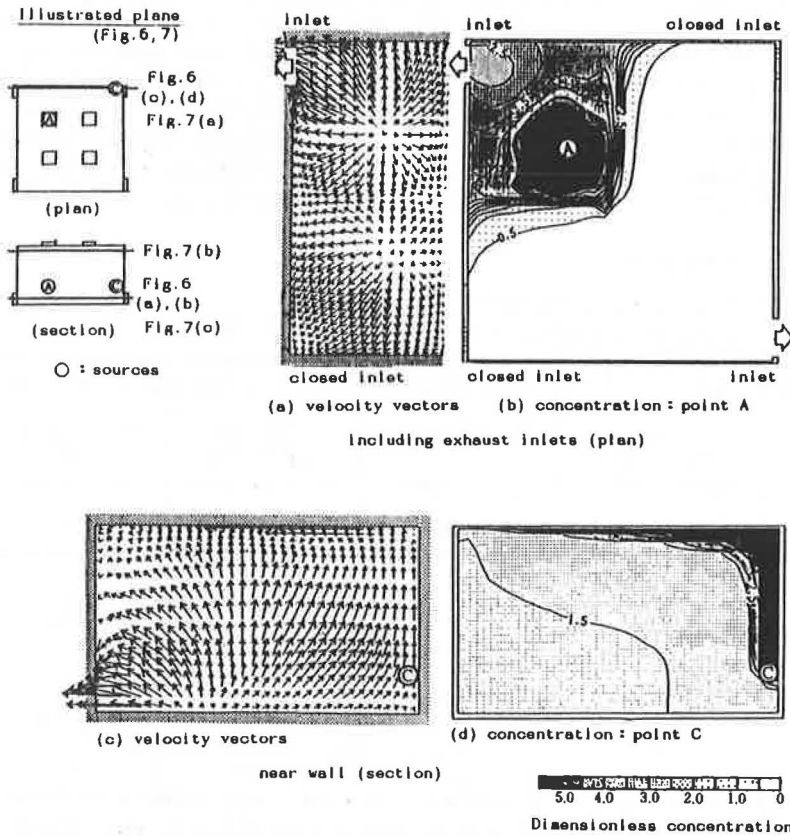


Figure 6 Velocity vectors and contaminant distribution (model 1) in TYPE 8 (4 outlets & 2 inlets)

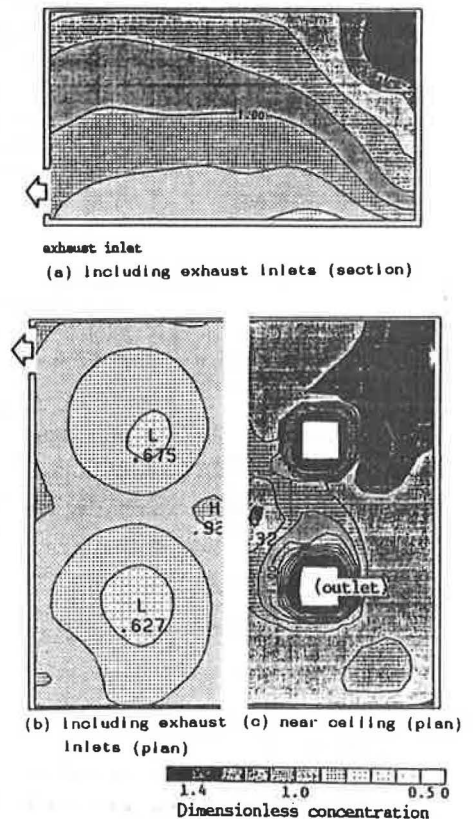


Figure 7 Contaminant distribution (SVE3) in TYPE 8 (4 outlets & 2 inlets, source: uniform generation in whole room)

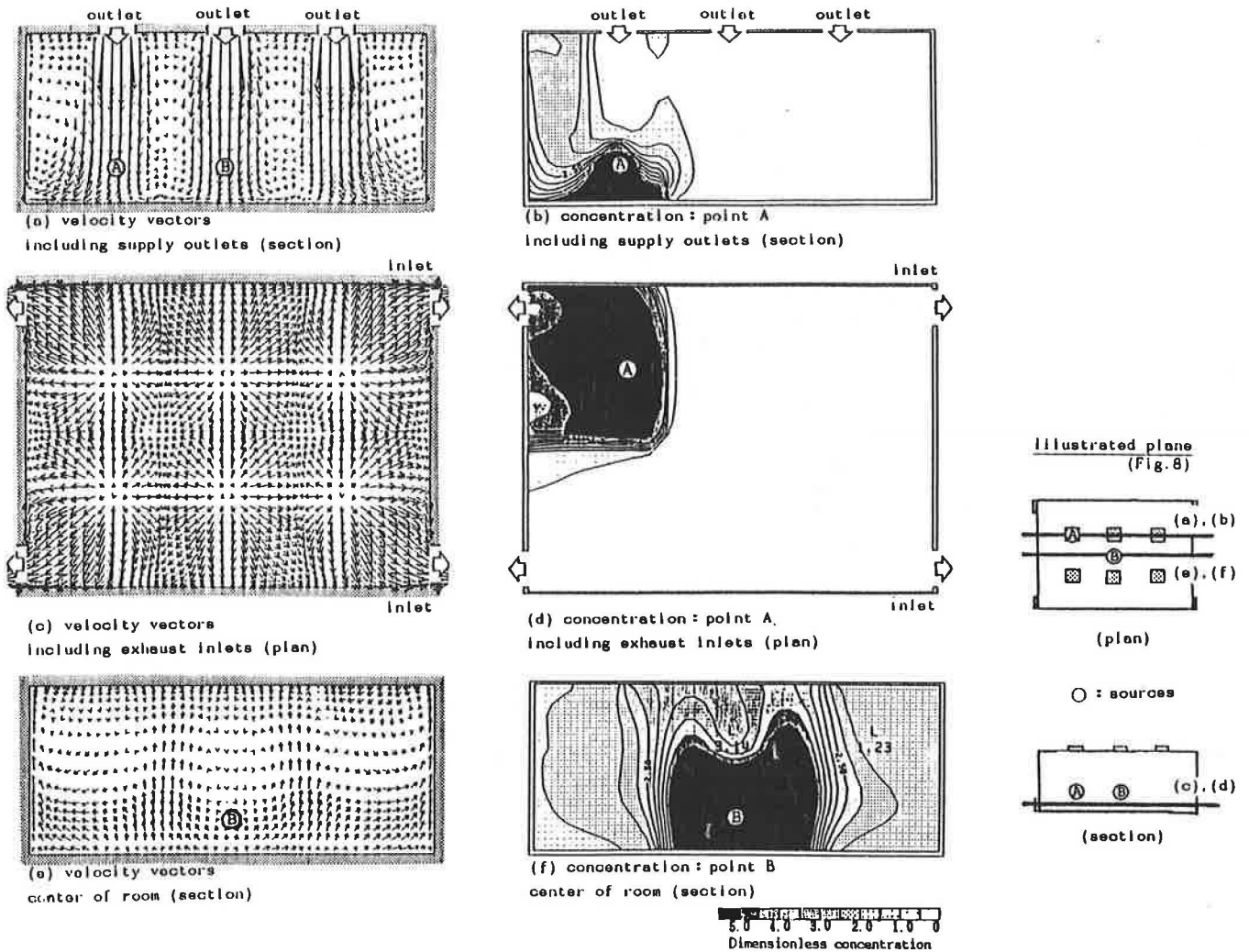


Figure 8 Velocity vectors and contaminant distribution (model 1) in TYPE 3 (6 outlets & 4 inlets, source: point A, B)

The concentration in the case of uniform contaminant generation throughout the room remains very high at the upper side of the room, at each corner of the room, and at the area around the supply outlets (cf. Figure 10), where the possibility of the air mass being contaminated becomes very high because of its long traveling time from the supply outlets.

DISCUSSION

The influence of the arrangement of the supply and exhaust openings on the flow and contaminant diffusion fields is summarized as follows:

The flow fields in such rooms as analyzed here are well modeled as combinations of flow units, each of which is composed of one supply jet and the rising streams around it. When the number of supply outlets is decreased, the flow units corresponding to the eliminated supply outlets vanish and the adjacent remaining flow units expand. When the contaminant is generated in that expanding flow unit, contaminant spreads throughout the flow unit and the value of the mean radius of diffusion becomes greater.

While the change of arrangement of the exhaust inlets has a small affect on the entire flow field, it does have a large influence on the contaminant diffusion field. When

the two exhaust inlets at the corner of the room are eliminated, rising streams along the walls grow stronger in front of the eliminated exhaust inlets. Since these areas are located far from the remaining exhaust inlets, the contaminant generated in this area is exhausted less effectively from the room. The fresh air mass takes a long time traveling to these areas, and the possibility for it to be contaminated becomes large.

Raising the location of the exhaust inlet has little influence on the flow field except for the area near the exhaust inlet.

INFLUENCE OF SYSTEMATIC CHANGE OF ARRANGEMENT OF SUPPLY OUTLET (TYPE 4, 10-13)

When designing a clean room, a matter of great concern is how the air exchange rate is to be set because it is directly related to operating expense. In this section, flow and contaminant diffusion fields in the same room with different arrangements of supply outlets (Type 4, 10-13) are compared. These supply arrangements, in which the numbers are progressively decreased, are modeled on the basis that the air exchange rate is decreased by the elimination of supply outlets rather than by decreasing the

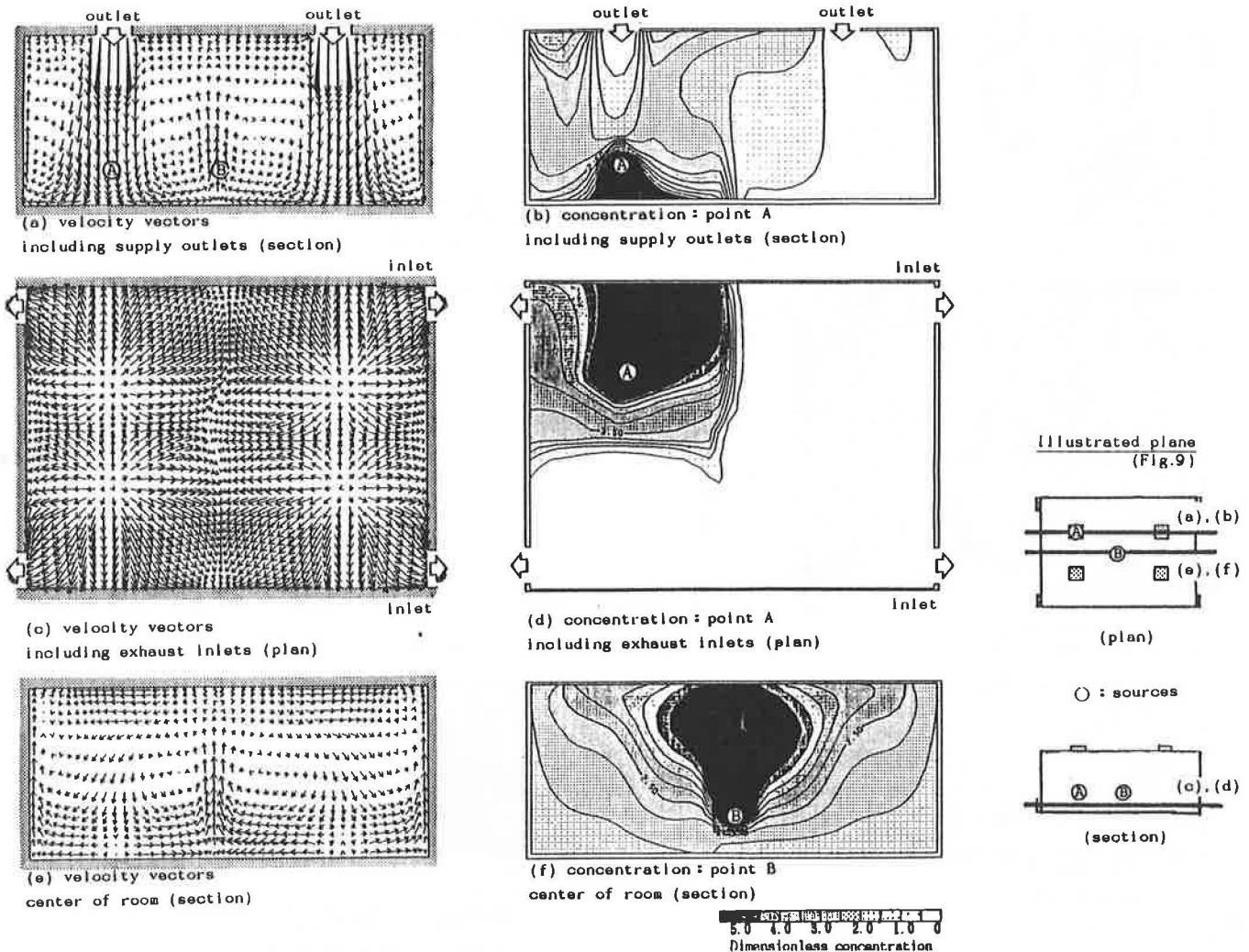


Figure 9 Velocity vectors and contaminant distribution (model 1) in TYPE 9 (4 outlets & 4 inlets, source: point A, B)

supply air volume.

Figure 11 shows the flow field and contaminant diffusion field in the case where the contaminant is generated at the center of the room (Point E). The outline of the structure of the flow units is illustrated in each figure using broken lines. It must be noted that in these figures the dimensionless concentration Model 1 is used.

Flowfields and Contaminant Diffusion Fields in Case of Contaminant Generated at E

Type 4 (Figures 11a-c). There are nine flow units in the room model, and rising streams appear at the boundary of each flow unit. The rising streams in the space between the two closest jets do not reach to the ceiling. Since the contaminant is generated in a supply jet, the highly contaminated region spreads under source point E. The flow unit that includes the contaminant source is highly contaminated.

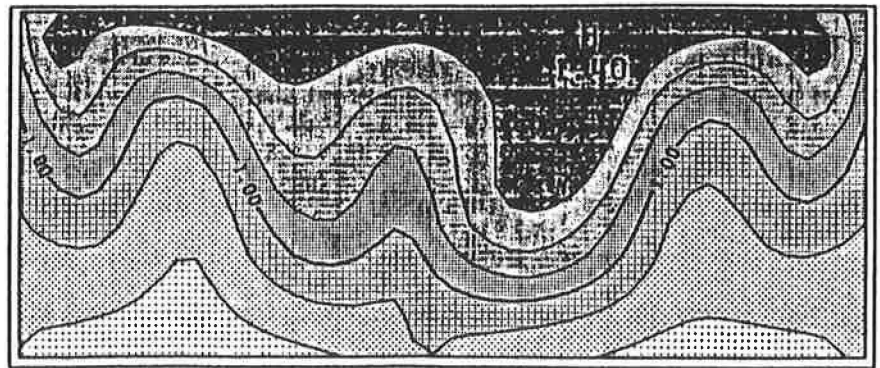
Type 10 (Figures 11d-f). Six flow units comprise the total flow field. At the centerline of the room, where three supply openings are closed, strong rising streams appear toward the ceiling. This centerline corresponds to the boundary of the expanded flow units. Since the contami-

nant is generated in this rising stream, the highly contaminated region spreads upward from source point E. The whole room is filled with highly contaminated air.

Type 11 (Figures 11g-i). The five checkered flow units comprise the total flow field. The rising streams surrounding the center flow unit spread toward the upper portion of the walls. Since the contaminants are generated in the supply jet in the center flow unit, the highly contaminated region appears under source point E. This contaminated air is transported by the rising flow toward the upper portion of the walls and most of the space becomes contaminated. The concentration becomes more than 1.0 in most of the space.

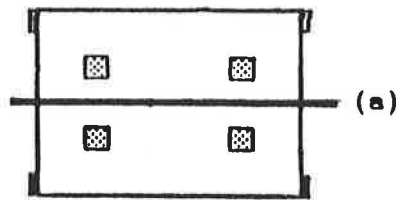
Type 12 (Figures 11j-l). Four large flow units comprise the total flow field. At the center of the room, a narrow rising stream appears toward the ceiling. Since the contaminant is generated in the rising stream, the highly contaminated region spreads above source point E, and most of the room is filled with contaminated air. In this simulation, the contaminant diffusion field is slightly asymmetric because of the asymmetry of the flow field due to numerical instability.

Type 13 (Figures 11m-o). There is only one flow unit

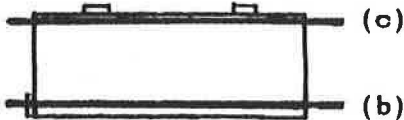


(a) center of room (section)

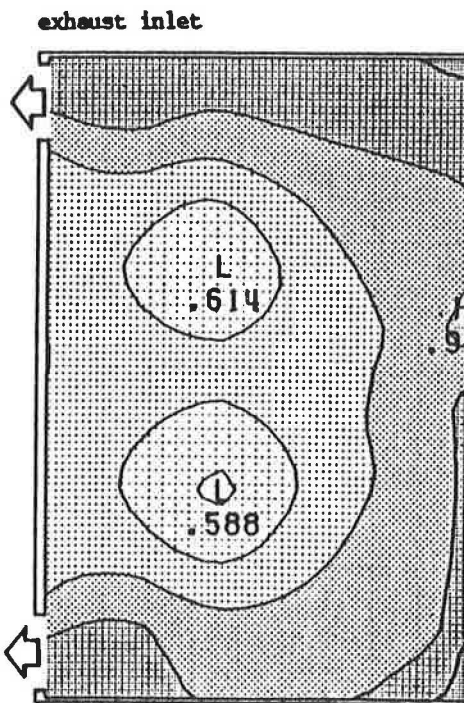
Illustrated plane
(Fig.10)



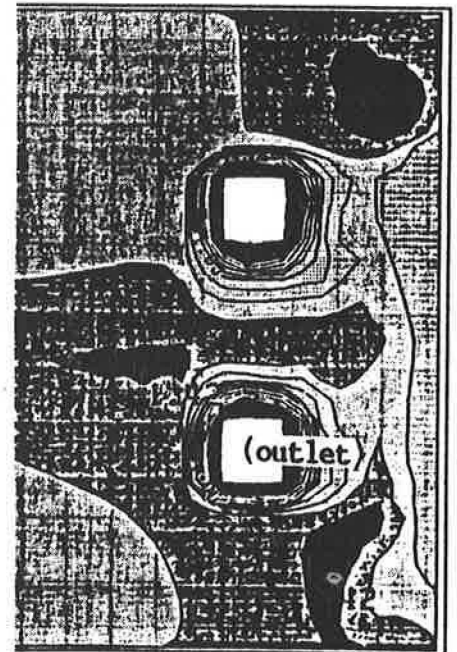
plan of TYPE 9



section of TYPE 9



(b) including exhaust inlets (plan)



(c) near ceiling (plan)

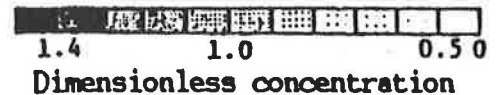


Figure 10 Contaminant distribution (SVE3) in TYPE 9 (4 outlets & 4 inlets, source: uniform generation in whole room)

in the room model. Since the contaminant is generated in the supply jet, the highly contaminated region spreads under source point E. The concentration is more than 1.5 throughout the whole room except for the area around the clean supply jet.

Comparison of Location of Supply Outlets concerning Ventilation Effectiveness (Source Point E)

In Table 6 two kinds of averaged spatial concentration (Models 1 and 2) and the mean radius of diffusion are tabulated for each type. Model 1 is a dimensionless con-

centration, which is normalized by the averaged concentration, C_0 , for all exhaust inlets for each type. Model 2 is also a dimensionless concentration, converted so as to have the same contaminant generation rate as Type 4 despite the different air exchange rate.

The supply air velocity is the same for all types. Therefore, the air exchange rate is naturally different for each. In Model 1, the generation rate differs and, naturally, the ratio of contaminant generation to air supply rate, the representative concentration (C_r) used in dimensionless value, is also not the same. But in Model 2, the generation rate is modified to be the same for all types. In that case the representative concentration, C_r , of Type 4 is used in

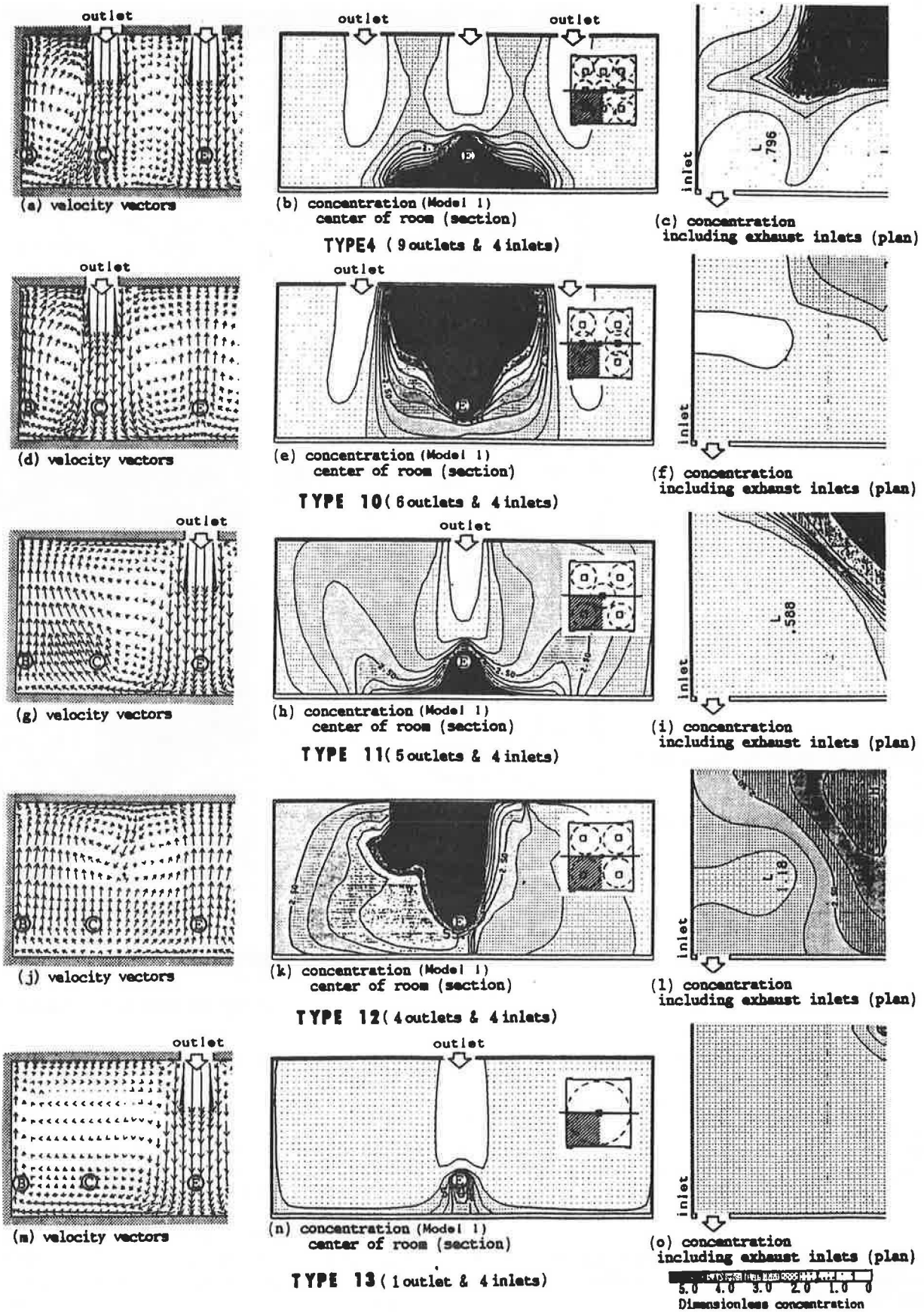
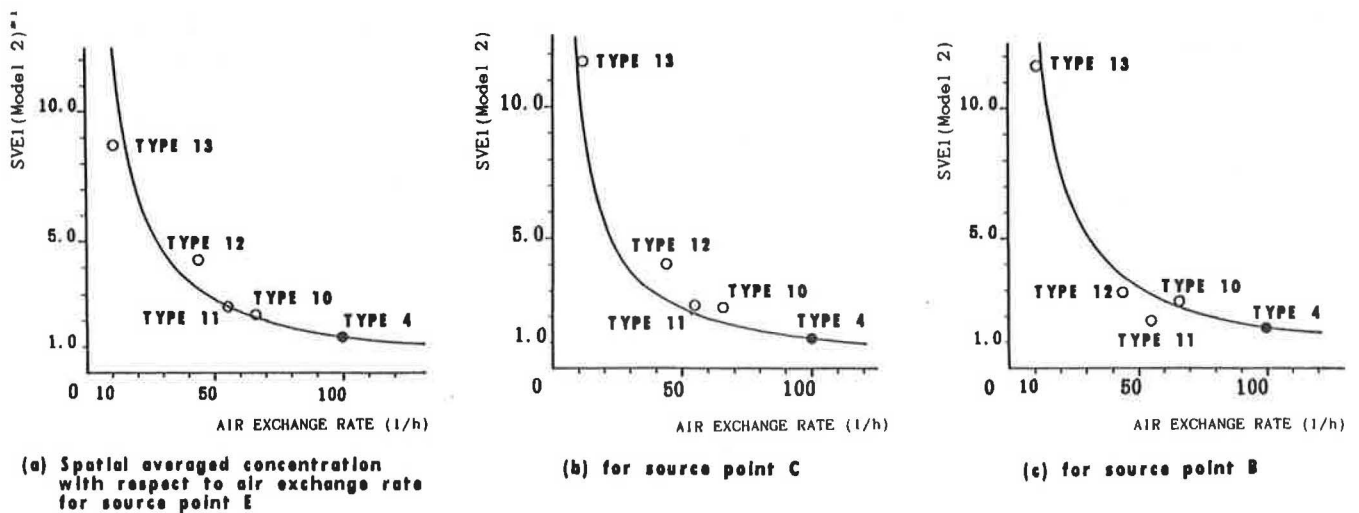


Figure 11 Effect of decreasing supply opening on diffusion field (TYPE 4, TYPE 10-13, source: point E)



*1 SVE1 : spatial averaged concentration. Model 2 : cf. Table 5
 *2 Contaminant generation rate for each type is same as in TYPE 4.

Figure 12 Comparisons of ventilation efficiency based on SVE1 by decreasing supply openings

common for making the dimensionless value.

Figure 12a shows the spatial average concentration of each type for source point E. In this figure, the dimensionless concentration of Model 2 is shown. The hyperbolic curve expresses the dimensionless average spatial concentration of Type 4 in which the air exchange rate is gradually decreased under the condition of a constant generation rate. We can thus comprehend the ventilation effectiveness of the different arrangements of the supply outlets. Using this figure, if the plotted point of average spatial concentration for a type is below the hyperbolic curve, the ventilation effectiveness of that type is superior to that of Type 4 under the same air exchange rate. This corresponds to the comparison based on Model 1, since the comparison based on Model 1 assumes the same air exchange rate and the same contaminant generation rate.

Since the plotted points of the spatial averaged concentration of Type 10 and Type 11 are on the hyperbolic curve, it may be concluded that the arrangements of the

supply outlets given as Type 10 and Type 11 have an effective ventilation ability equal to that of Type 4 for the same air exchange rate. The ventilation effectiveness of Type 12 is inferior to that of Type 4 because its plotted point is above the hyperbolic curve. Although the value of the average spatial concentration of Type 13 is rather large, in accord with its correspondingly small air exchange rate, the contaminant-exhausting ability is somewhat superior to Type 4 in the same air exchange rate. In conclusion, for the contaminant source point E, ventilation effectiveness among these different supply outlet arrangements may be judged in the following order: Type 13 > Type 4 > Type 11 > Type 10 > Type 12 (cf. comparison of SVE 1 based on Model 1 in Table 6).

For the mean radius of diffusion Type 4, Type 11, and Type 13 have rather high values (cf. Table 6). The contaminant source point in all these cases is located in the supply jet.

TABLE 6
 Values of Spatial Averaged Concentration (SVE1) and Mean Radius of Diffusion (SVE2) for TYPE 4, TYPE 10 ~ 13

sources	point E (center of room)			point C (between center and wall)			point B (near the wall)		
	SVE1 (Model 1)	SVE1 (Model 2)*1	SVE2 (*2)	SVE1 (Model 1)	SVE1 (Model 2)	SVE2	SVE1 (Model 1)	SVE1 (Model 2)	SVE2
TYPE 4	1.37	1.37	4.2	1.15	1.15	3.3	1.56	1.56	3.1
TYPE 10	1.51	2.27	4.0	1.56	2.34	4.1	1.68	2.52	4.0
TYPE 11	1.40	2.52	4.3	1.38	2.48	3.8	1.03	1.85	4.0
TYPE 12	1.92	4.32	3.8	1.81	4.07	3.8	1.30	2.90	4.0
TYPE 13	0.97	8.73	3.9	1.31	11.76	4.3	1.29	11.58	4.3

*1 : Model 2 is also dimensionless concentration in which contaminant generation rate is the same as TYPE 4 for all types.
 *2 : Dimensionless length: these values are made dimensionless by dividing by the width of the supply outlet (0.6m).

Diffusion Field in Case of Contaminant Generated at C (Type 4, 10-13)

Because contaminant source point C is located in the supply jet in the case of Type 4 and Type 10 (cf. Figures 11a and 11d), the highly contaminated region spreads under the source point. Furthermore, contaminated air is transported toward the ceiling by strong rising streams along the wall and the highly contaminated region spreads along the wall. In the case of Type 11 (cf. Figure 11g), slanted streams rise from around source point C toward the upper portion of the wall. In the case of Type 12 (cf. Figure 11j), wide streams rise from the floor to the ceiling from around source point C. In the case of Type 13 (cf. Figure 11m), horizontal streams along the floor appear around source point C, and the highly contaminated region spreads along these adjective flows from the source point. Contaminant spreads both in the flow unit in which the contaminant is generated and in the adjacent flow units located between the contaminant source and the closest exhaust inlet. In the case of Type 4, the contaminant spreads through one-third of the room, while in other cases it occupies about half the room except for Type 13. In Type 13, the contaminant spreads into the entire space.

Comparison of Location of Supply Outlets Concerning Ventilation Effectiveness (Source Point C)

For the case of source point C, two kinds of average spatial concentration (Models 1 and 2) and the mean radius of diffusion are tabulated for each type in Table 6 and comparisons of ventilation effectiveness are shown in Figure 12b in the same manner as before.

Since every plotted point of the average spatial concentration in Type 10—Type 13 room model is above the hyperbolic curve, it may be concluded that the arrangement of the supply outlets in Type 10—Type 13 for this contaminant source is inferior to that of Type 4 under the same air exchange rate. For contaminant source point C, ventilation effectiveness among these different cases of arrangement of supply outlets is estimated in the following order: Type 4 > Type 13 = Type 11 > Type 10 > Type 12.

For the values of the mean radius of diffusion, there seems to be small difference among them.

Diffusion Field in Case of Contaminant Generated at B (Type 4, 10-13)

Source point B is placed near the wall. In every type, strong rising streams appear along the wall (cf. Figures 11a, d, g, j, and m). The contaminant generated at source point B is transported by this rising stream, and the contaminated area spreads widely from the source point to the ceiling.

The contaminants spread in the flow unit that contains the contaminant source and some spread in the adjacent flow units, which are located between the contaminant source and the closest exhaust inlet. In the case of Type 4, about one-third of the room is highly contaminated, while in the other cases about one-half of the room is contaminated.

Comparison of Location of Supply Outlets concerning Ventilation Effectiveness (Source Point B)

For the case of source point B, two kinds of average spatial concentration and the mean radius of diffusion are tabulated for each type in Table 6; comparisons of ventilation effectiveness are shown in Figure 12c as before.

Since the plotted points of the averaged spatial concentration of Type 11 and Type 12 are below the hyperbolic curve, it may be concluded that for this contaminant source, the arrangements of the supply outlets in Type 11 and Type 12 are superior to that of Type 4 under the same air exchange rate from the viewpoint of ventilation effectiveness. Note especially that Type 11, which has only five-ninths the air exchange rate of Type 4, has almost equal ventilation effectiveness with Type 4. Thus, for contaminant source point B, ventilation effectiveness among these different arrangements of supply outlets is estimated in the following order: Type 11 ≧ Type 13 > Type 12 > Type 4 > Type 10.

The values of the mean radius of diffusion for these room models, except for Type 4, are close to 4.0 and thus larger than Type 4 (3.1: cf. Table 6).

DISCUSSION

Flow fields and diffusion fields (Model 2) are compared among Type 4 and Type 10—Type 13 clean rooms in which the arrangement and the numbers of supply outlets vary. Type 4 has the most effective ventilation ability, and Type 13 has the worst ventilation ability because the former has the largest air exchange rate and the latter has the smallest value. However, when a comparison is made based on dimensionless concentration Model 1, which means that it is made assuming of the same air exchange rate and the same generation rate, the arrangement the supply outlets that has the most effective ventilation ability differs in accord with the position of the contaminant source.

For the three cases of contaminant source analyzed here, the ventilation ability of Type 11 is relatively effective because its five supply outlets and resultant five flow units are in a checkered arrangement with clear boundaries.

CONCLUSION

Flow fields and contamination diffusion fields in several types of conventional-flow-type clean rooms are analyzed by means of numerical simulation based on the $k - \epsilon$ two-equation model. In these analyses, the influence of the arrangement of supply outlets and exhaust inlets on flow fields and contaminant diffusion fields is clarified. The results are as follows:

1. Numerical simulation easily and precisely manifests complex conditions that cannot be realized in model experiments. Numerical simulation is the most useful method for analyzing parametrically the influence of changes in the flow conditions.

2. The supply outlets have great influence on the flow fields and also a rather large influence on contaminant diffusion fields. When the numbers of the supply outlets are decreased, the flow units corresponding to the eliminated supply outlets disappear and the remaining flow units expand.

3. The arrangement of exhaust inlets has a rather small influence on the flow fields. However, since the path of contaminant transportation is changed greatly by the position of the exhaust inlets, contaminant diffusion fields are likely to be affected greatly by the arrangements of the exhaust inlets.

4. The arrangement of the supply outlets in a checkered pattern is superior to the arrangement of the supply outlets in a linear pattern from the viewpoint of ventilation effectiveness in general.

NOMENCLATURE

C_μ, C_1, C_2	= empirical constants in $k-\epsilon$ turbulence model (cf. Table 2)
C	= mean contaminant concentration
C_o	= representative concentration defined by that of exhaust outlet
E	= empirical constant in log law, 9.0 in case of smooth wall
h	= interval of finite difference
h_1	= length from the solid wall surface to the center of the adjacent fluid cell
k	= turbulence kinetic energy
l	= length scale of turbulence
L_o	= representative length for non-dimensionalization defined by width of supply outlet
P	= mean pressure
q	= contaminant generation rate
Q	= air exchange volume
SVE	= scale for ventilation efficiency
U_i, U_j	= components of mean velocity vector
U_o	= representative velocity for non-dimensionalization defined by inflow jet velocity
ϵ	= turbulence dissipation rate
κ	= von Karman constant, 0.4
ρ	= fluid density
ν	= molecular kinematic viscosity
ν_T	= eddy kinematic viscosity

$\sigma_1, \sigma_2, \sigma_3$ = turbulence Prandtl/Schmidt number of k, ϵ, C (cf. Table 2)

ACKNOWLEDGMENTS

This study has been partially supported by a grant-in-aid for scientific research from the Japanese Ministry of Education, Culture and Science.

REFERENCES

- Chieng, C.C., and Launder, B.E. 1980. "On the calculation of turbulent heat transport downstream from an abrupt pipe expansion." *Numerical Heat Transfer*, Vol. 3, pp. 189-207.
- Kato, S., and Murakami, S. 1988a. "New ventilation efficiency scales based on spatial distribution of contaminant concentration aided by numerical simulation." *ASHRAE Transactions*, Vol. 94, Part 2, pp. 309-330.
- Kato, S.; Murakami, S.; and Nagano, S. 1988b. "Study on diagnostic system for simulation of turbulent flow in room (Part 17). Investigation on each type wall boundary of $k-\epsilon$ 2-equation model (No. 1)." *Transactions of annual meeting of SHASEJ*, pp. 573-576.
- Launder, B.E., and Spalding, D.B. 1974. "The numerical computation of turbulent flows." *Computer Methods in Applied Mechanics and Engineering*, Vol. 3, pp. 269-289.
- Nagano, S.; Murakami, S.; and Kato, S. 1988. "Study on diagnostic system for simulation of turbulent flow in room (Part 18). Investigation on each type wall boundary of $k-\epsilon$ 2-equation model (No. 2)." *Transactions of annual meeting of SHASEJ*, pp. 577-580.
- Murakami, S.; Kato, S.; and Suyama, Y. 1987. "Three-dimensional numerical simulation of turbulent airflow in a ventilated room by means of a two-equation model." *ASHRAE Transactions*, Vol. 93, Part 2, pp. 621-642.
- Murakami, S.; Kato, S.; and Suyama, Y. 1988. "Numerical and experimental study on turbulent diffusion fields in conventional flow type clean rooms." *ASHRAE Transactions*, Vol. 94, Part 2, pp. 469-493.
- Rodi, W. 1984. "Turbulence models and their application in hydraulics." *IAHR*. The Netherlands.

